Novel Bifunctional Viologen−Linked Pyrene Conjugates: Synthesis and Study of Their Interactions with Nucleosides and DNA

ARTICLE *in* THE JOURNAL OF PHYSICAL CHEMISTRY B · JANUARY 2007

Impact Factor: 3.3 · DOI: 10.1021/jp063079o · Source: PubMed

3 AUTHORS, INCLUDING:

Mahesh Hariharan
Indian Institute Of Science Education and Re…
45 PUBLICATIONS **843** CITATIONS
SEE PROFILE

Joshy Joseph
Council of Scientific and Industrial Research …
32 PUBLICATIONS **448** CITATIONS
SEE PROFILE

Novel Bifunctional Viologen-Linked Pyrene Conjugates: Synthesis and Study of Their Interactions with Nucleosides and DNA

Mahesh Hariharan, Joshy Joseph, and Danaboyina Ramaiah*

Photosciences and Photonics, Chemical Sciences and Technology Division, Regional Research Laboratory, Council of Scientific and Industrial Research, Trivandrum 695 019, India

Received: May 19, 2006; In Final Form: September 27, 2006

With the objective of developing efficient DNA oxidizing agents, a new series of viologen-linked pyrene conjugates with the general formula **PYL*n*V**$^{2+}$, having a different number of methylene spacer units (**L***n*) was synthesized, and their interactions with nucleosides and DNA have been investigated through photophysical and biophysical techniques. The viologen-linked pyrene derivatives **PYL1V**$^{2+}$ ($n = 1$), **PYL7V**$^{2+}$ ($n = 7$), and **PYL12V**$^{2+}$ ($n = 12$) exhibited characteristic fluorescence emission of the pyrene chromophore centered around 380 nm but with significantly reduced yields when compared to those of the model compound **PYL1Et$_3$**$^{+}$. The fluorescence quenching observed in these systems is explained through an electron-transfer mechanism based on a calculated favorable change in free energy ($\Delta G_{ET} = -1.59$ eV), and the redox species characterized through laser flash photolysis studies. Intramolecular electron-transfer rate constants (k_{ET}) were calculated from the observed fluorescence yields, and the singlet lifetimes of the model compound and are found to decrease with increasing spacer length. The DNA binding studies of these systems through photophysical, chiroptical, and viscometric techniques demonstrated that these systems effectively undergo DNA intercalation with association constants (K_{DNA}) in the range of $1.1-2.6 \times 10^4$ M^{-1} and exhibit 2:1 sequence selectivity for poly(dG)·poly(dC) over poly(dA)·poly(dT). Photoactivation of these systems initiates electron transfer from the singlet excited state of the pyrene chromophore to the viologen moiety followed by an electron transfer from DNA to the oxidized pyrene. This results in the formation of stable charge-separated species such as radical cations of both DNA and reduced viologen as characterized by laser flash photolysis studies and subsequently the oxidized DNA modifications. These novel systems are soluble in buffer media, stable under irradiation conditions, and oxidize DNA efficiently and selectively through a cosensitization mechanism and hence can be useful as photoactivated DNA cleaving agents.

1. Introduction

Design of functional molecules that bind selectively to DNA and are capable of modifying duplex or single-stranded DNA is an active area of research that has important biochemical and medicinal applications.[1] Several molecules, which induce DNA modifications by various mechanisms, have been reported in the literature.[2] Among these, the photoactivated DNA oxidizing agents have been found to possess significant practical advantages over the reagents that cleave DNA under thermal conditions.[3] An interesting aspect of these agents is that they allow the reaction to be controlled spatially and temporally by combining all of the components of the reaction mixture before the irradiation. Excitation of the reaction mixture with an appropriate light source initiates the reaction, which continues until the light is shut off.[4,5] The ability to control light in both spatial and temporal senses would be advantageous for various biological applications.

By absorption of light, these reagents are known to modify DNA through different mechanisms, including the electron-transfer reaction, generation of diffusible and nondiffusible reactive intermediates, and hydrogen atom abstraction.[3−6] In the latter two processes, selectivity of the DNA cleavage is rather difficult to attain, as these reactions are generally nonspecific, while the former mechanism is shown to have base selectivity. A large number of simple organic as well as inorganic sensitizers have been reported that oxidize DNA through a photoinduced electron-transfer mechanism.[7,8] However, most of these sensitizers were found to be less efficient due to the existence of efficient electron back-transfer between the resultant oxidized DNA and the reduced sensitizer. To overcome the drawbacks of the electron back-transfer process associated with such systems, a few examples based on a cosensitization mechanism have been developed.[9,10] These systems consist of a sensitizer, which is also an intercalator, that transfers an electron upon excitation to a cosensitizer (electron acceptor), which is bound on the surface of DNA. The photosensitization involving the cosensitizer that bound far away from the sensitizer is expected to inhibit the electron back-transfer and thereby increase the DNA modifications. However, in reality, only a marginal improvement in DNA oxidation was observed using these systems owing to the complications with respect to the concentration, distance, and DNA binding affinities of the sensitizer and cosensitizer. Therefore, molecules that exhibit considerable DNA binding affinity and specificity in cleavage are yet to be achieved.

Recently, we have reported DNA binding and cleaving efficiencies of a few bifunctional conjugates consisting of acridine as the sensitizer and the viologen moiety as the cosensitizer.[11] These molecules exhibited a high affinity for

* Author to whom correspondence should be addressed. Phone: (+91) 471 2515362. Fax: (+91) 471 2490186 or 2491712. E-mail: rama@csrrltrd.ren.nic.in or d_ramaiah@rediffmail.com.

10.1021/jp063079o CCC: $33.50
Published on Web 11/09/2006

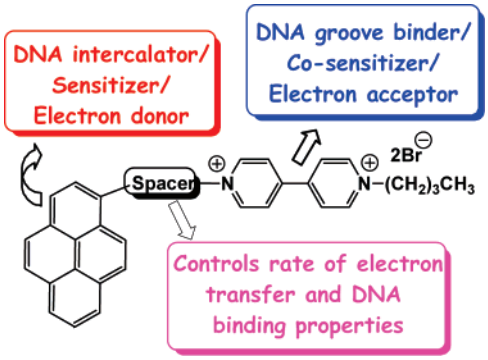

Figure 1. Schematic representation of the cosensitization strategy adopted for the design of the photoactivated DNA cleaving agents.

DNA and induced DNA damage that is characteristic of an electron-transfer mechanism involving two different pathways. One of these pathways follows the oxidation of DNA by the excited state of acridine, whereas the other one involves the oxidation of DNA by the charge-separated viologen-linked acridine. Eventhough both these pathways lead to the oxidation of DNA, electron back-transfer from the excited acridine to DNA involved in the former pathway reduces the efficiency of the DNA damage. Progress in this area would require new strategies to control the sequence of electron-transfer reactions between the donor−acceptor dyads and the DNA bases and the efficient oxidation of DNA through a cosensitization mechanism.

In this context, we have designed a new series of donor−acceptor conjugates that can strongly bind to DNA and, in principle, can oxidize DNA selectively through a cosensitization mechanism (Figure 1). We chose pyrene, a known intercalator, as the electron donor, whereas the viologen moiety, a groove binder, was chosen as the electron acceptor. These bifunctional molecules were designed on the basis of theoretically calculated changes in the free energy values for the electron-transfer and intermolecular fluorescence quenching studies. Herein, we report the synthesis, photophysical and DNA binding properties, and inter- and intramolecular electron-transfer reactions of a few novel bifunctional viologen-linked pyrene conjugates (Scheme 1). Our results demonstrate that the pyrene moiety in these molecules constitutes an interesting variation and plays a major role in controlling the electron-transfer pathways, which lead to the efficient photooxidation of DNA.

2. Experimental Section

2.1. General Techniques. The equipment and procedure for melting point determination and spectral recordings are described in earlier publications.[12,13] An Elico pH meter was used for pH measurements. The electronic absorption spectra were recorded on a Shimadzu UV−vis−near-IR spectrophotometer. Fluorescence spectra were recorded on a SPEX-Fluorolog F112X spectrofluorimeter. The fluorescence quantum yields were determined by using optically matched solutions. Quinine sulfate ($\Phi_f = 0.54$) in 0.1 N H_2SO_4 was used as the standard.[14] Fluorescence lifetimes were measured using a IBH picosecond single photon counting system. The fluorescence decay profiles were deconvoluted using IBH data station software, version 2.1, and fitted with a monoexponential decay and minimizing the χ^2 values of the fit to 1 ± 0.1. The quenching rate constant k_q was calculated by employing eqs 1 and 2, where I_0 and I are the fluorescence intensities in the absence and presence of quencher (Q), K_{SV} is the Stern−Volmer constant, and τ_0 is the singlet lifetime of 1-(hydroxylmethyl)pyrene in the absence of quencher

$$\frac{I_0}{I} = 1 + K_{SV}[Q] \quad (1)$$

$$K_{SV} = K_q \tau_0 \quad (2)$$

From the relative fluorescence quantum yields of the viologen-linked pyrene derivatives and fluorescence lifetime of the

SCHEME 1: Synthesis of the Model Compound PYL1Et$_3^+$ and the Bifunctional Viologen-Linked Pyrene Conjugates PYL1V^{2+}, PYL7V^{2+}, and PYL12V^{2+}.

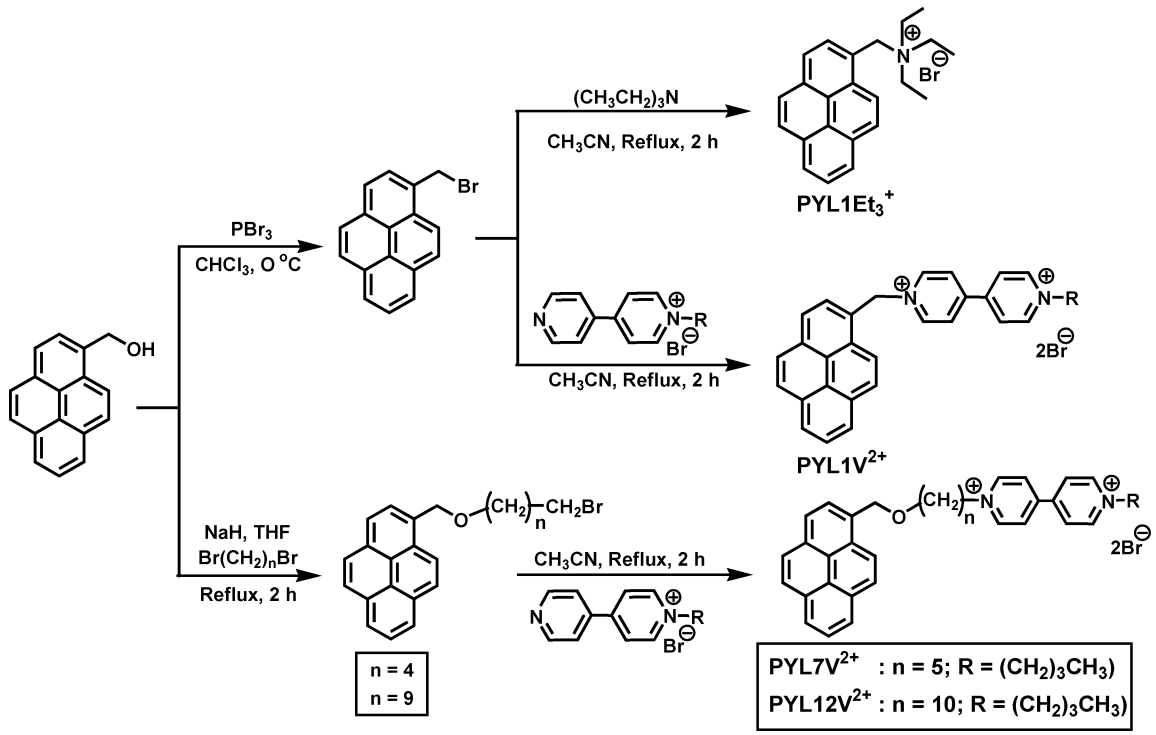

model derivative **PYL1Et$_3$**$^+$, an estimate of the rate constant of the electron-transfer process k_{ET} can be made by using eq 3

$$k_{ET} = \frac{(\Phi_{ref}/\Phi) - 1}{\tau_{ref}} \quad (3)$$

where Φ_{ref} and Φ are the relative fluorescence quantum yields of the model compound **PYL1Et$_3$**$^+$ and the viologen-linked pyrene derivative, respectively, and τ_{ref} is the fluorescence lifetime of the model compound **PYL1Et$_3$**$^+$. Laser flash photolysis experiments were carried out in an Applied Photophysics model LKS-20 laser kinetic spectrometer using the third harmonic (355 nm) of a Quanta Ray GCR-12 series pulsed Nd:YAG laser. Doubly distilled water was used in all the studies. ^{1}H and ^{13}C NMR were measured on a 300 MHz Bruker advanced DPX spectrometer.

A solution of calf thymus (CT) DNA was sonicated for 1 h to minimize the complexities arising from DNA flexibility[15] and filtered through a 0.45 μm Millipore filter ($M_w = 3 \times 10^5$ g mol^{-1}). The concentrations of DNA solutions were determined by using the average value of 6600 M^{-1} cm^{-1} for the extinction coefficient of a single nucleotide at 260 nm.[16] Polynucleotides were dissolved in phosphate buffer, and the concentrations were determined by using the average extinction coefficient value of 7400 M^{-1} cm^{-1} at 253 nm for poly(dG)·poly(dC) and 6000 M^{-1} cm^{-1} at 260 nm for poly(dA)·poly(dT).[16] Viscosity measurements of DNA were carried out using CT DNA (0.88 mM) in phosphate buffer (10 mM) containing 2 mM NaCl (pH 7.4) at 25 °C and also in the presence of various viologen-linked pyrene derivatives and model derivatives under similar conditions.

The DNA binding studies were carried out in 10 mM phosphate buffer (pH 7.4) containing 2, 100, and 500 mM NaCl. The intrinsic binding constant of the viologen-linked pyrene derivatives with CT DNA was determined using absorbance at 344 nm recorded after each addition of CT DNA. The intrinsic binding constant K_{DNA} was determined from the half-reciprocal plot of $D/\Delta\epsilon_{ap}$ versus D, where D is the concentration of DNA in base pairs, $\Delta\epsilon_{ap} = [\epsilon_a - \epsilon_F]$, and $\Delta\epsilon = [\epsilon_b - \epsilon_F]$.[17] The apparent extinction coefficient, ϵ_a, is obtained by calculating $A_{[obsd]}$/[pyrene derivatives]. ϵ_b and ϵ_F correspond to the extinction coefficient of the bound form of the pyrene derivatives and the extinction coefficient of the free pyrene derivatives, respectively. The data were fitted to eq 4

$$\frac{D}{\Delta\epsilon_{ap}} = \frac{D}{\Delta\epsilon} + \frac{1}{\Delta\epsilon K_{DNA}} \quad (4)$$

with a slope equal to $1/\Delta\epsilon$ and a y-intercept equal to $1/(\Delta\epsilon K_{DNA})$. ϵ_b was determined from $\Delta\epsilon$, and K_{DNA} was obtained from the ratio of the slope to the y-intercept. The binding site size, n, of the viologen-linked pyrenes was evaluated by carrying out DNA binding studies at an ionic strength of 10 mM phosphate buffer. The intersection of the two straight lines drawn through the linear portions of the absorption titration curve gave the binding site size, n, for the corresponding viologen-linked pyrene conjugate.

The counterion release that accompanies the binding of a ligand to DNA can be obtained from the slope of log K_{DNA} versus $-\log[Na^+]$[18] according to eq 5

$$\frac{-\delta \log K_{DNA}}{\delta \log [Na^+]} = -Z\Psi \quad (5)$$

where Z is charge of the ligand and Ψ represents the average number of condensed and screened sodium ions associated with the DNA phosphate group. The nonelectrostatic contributions to the association of ligand with DNA can be obtained from eq 6

$$\ln K_{DNA} = \ln K_T^{\,0} + Z\xi^{-1} \ln(\gamma_{\pm}\delta) - Z\Psi \ln[Na^+] \quad (6)$$

where K_T^0 is the equilibrium constant that does not include the free energy of ion release. For the B-form of DNA, the dimensionless polymer charge density ξ is 4.2. The variable δ is 0.33b, where b is the average axial charge spacing, 1.7 Å for B-form of DNA. The mean activity coefficient at an appropriate salt concentration is $\gamma \pm 0.78$ at 100 mM NaCl.

2.2. Materials. 1-(Hydroxymethyl)pyrene, 4,4′-bipyridine, 1,5-dibromopentane, 1,10-dibromodecane, 1-bromobutane, triethanolamine, guanosine, adenosine, thymidine, and cytidine (all from Aldrich), CT DNA (Pharmacia Biotech), and polynucleotides (Amersham Pharmacia Biotech, Inc.) were obtained and used as received. 1-Butyl-4,4′-bipyridinium bromide was obtained in 95% yield by the reaction of 4,4′-bipyridine with 1-bromobutane in the molar ratio of 3:1 in dry acetonitrile.[11] The petroleum ether used was the fraction with a boiling point of 60−80 °C.

2.3. Synthesis of 1-[(Pyren-1-yl)methyl]-1′-*N*,*N*′,*N*″-triethylammonium Bromide (PYL1Et$_3$ $^+$**).** To an ice cold solution of 1-(hydroxymethyl)pyrene (0.65 mmol) in 35 mL of dry chloroform, phosphorus tribromide (0.21 mmol) was added, and the resulting solution was stirred for 12 h. The reaction mixture was neutralized with saturated sodium bicarbonate solution. The organic layer was separated and evaporated under reduced pressure to give an 82% yield of 1-(bromomethyl)pyrene, after recrystallization from chloroform, mp 136−137 °C. ^{1}H NMR ($CDCl_3$, 300 MHz): δ 5.25 (2H, s), 8.06−8.13 (5H, m), 8.20−8.26 (3H, m), 8.37−8.40 (1H, d, $J = 9.2$ Hz). ^{13}C NMR ($CDCl_3$, 75 MHz): δ 32.2, 122.8, 124.8, 125.6, 126.2, 127.3, 127.7, 127.9, 128.2. Anal. Calcd for $C_{17}H_{11}Br$: C, 69.17; H, 3.76. Found: C, 69.31; H, 3.57.

To a solution of 1-(bromomethyl)pyrene (0.65 mmol) in dry acetonitrile (30 mL), triethylamine (0.65 mmol) was added and stirred for 12 h at room temperature. Precipitated product was filtered and dried in a vacuum oven to give a 45% yield of **PYL1Et$_3$**$^+$, which was recrystallized from a mixture (6:4) of methanol and ethyl acetate, mp 184−185 °C. ^{1}H NMR (DMSO-d_6, 300 MHz): δ 1.25−1.29 (9H, m), 3.35−3.42 (6H, m), 5.31 (2H, s), 8.17−8.73 (9H, m). ^{13}C NMR (DMSO-d_6, 75 MHz): δ 7.8, 52.7, 58.3, 121.0, 122.0, 122.9, 124.2, 125.4, 125.7, 126.1, 126.5, 128.3, 128.4, 129.3, 130.1, 130.9, 131.7. HRMS (ESI) Calcd for $C_{23}H_{26}BrN$: 396.3633. Found: 396.3639. Anal. Calcd for $C_{23}H_{26}BrN$: C, 69.70; H, 6.61; N, 3.53. Found: C, 69.59; H, 6.83; N, 3.71.

2.4. Synthesis of 1-[(Pyren-1-yl)methyl]-1′-butyl-4,4′-bipyridinium Dibromide (PYL1V^{2+}). To a solution of 1-(bromomethyl)pyrene (0.6 mmol) in dry acetonitrile (50 mL), 1-butyl-4,4′-bipyridinium bromide (0.6 mmol) was added and stirred at room temperature for 12 h. Precipitated product was filtered and dried to give a 29% yield of **PYL1V^{2+}**, which was recrystallized from a mixture (7:3) of methanol and ethyl acetate, mp 286−290 °C. ^{1}H NMR (DMSO-d_6, 300 MHz): δ 0.90−0.95 (3H, t, $J = 7.4$ Hz), 1.29−133 (2H, m), 1.93−1.97 (2H, m), 4.69 (2H, t, $J = 7.1$ Hz), 6.82 (2H, s), 8.17−8.75 (9H, m), 8.58−9.51 (8H, m). ^{13}C NMR (DMSO-d_6, 75 MHz): δ 13.8, 19.2, 33.2, 52.7, 61.8, 109.9, 115.4, 122.8, 124.1, 125.9, 126.6, 126.7, 126.8, 127.3, 127.4, 127.5, 127.7, 129.1, 129.5, 129.8, 130.6, 131.2, 146.2. HRMS (ESI) Calcd for $C_{31}H_{28}BrN_2$:

508.4715. Found: 508.4711. Anal. Calcd for $C_{31}H_{28}Br_2N_2$: C, 63.28; H, 4.80; N, 4.76. Found: C, 63.14; H, 4.69; N, 4.86.

2.5. Synthesis of {*N*-(Butyl)-*N*′-[5-(1-pyrenylmethoxy)pent-1-yl]}-4,4′-bipyridinium Dibromide (PYL7V^{2+}). To a stirred suspension of sodium hydride (19 mmol) in dry tetrahydrofuran (THF) (10 mL) under reflux conditions was added a solution of 1-(hydroxymethyl)pyrene (1 mmol) and 1,5-dibromopentane (5 mmol) over a period of 30 min in dry THF (20 mL). The reaction mixture was refluxed for 24 h, and excess sodium hydride was quenched with water. The organic layer was extracted with dichloromethane. Removal of the solvent under reduced pressure gave the product, which was purified by recrystallization from a mixture (2:8) of ethyl acetate and hexane to give a 53% yield, mp 83−84 °C. ^{1}H NMR ($CDCl_3$, 300 MHz): δ 1.20−1.80 (6H, m), 3.34−3.38 (2H, m), 3.59−3.63 (2H, m), 5.21 (2H, s), 7.98−8.38 (9H, m). ^{13}C NMR ($CDCl_3$, 300 MHz): δ 25.0, 29.0, 32.6, 33.7, 70.1, 76.6, 115.8, 123.5, 125.5, 125.2, 125.9, 126.9, 127.4, 127.6.

To a solution of 5-bromopentyl-1-methylpyrene ether (0.5 mmol) in dry acetonitrile (30 mL), 1-butyl-4,4′-bipyridinium bromide (0.5 mmol) was added and stirred for 12 h at room temperature. Precipitated product was filtered and dried in a vacuum oven to give the compound, which was then recrystallized from a mixture (7:3) of methanol and ethyl acetate, in a 32% yield, mp 216−217 °C. ^{1}H NMR (DMSO-d_6, 300 MHz): δ 0.94−2.08 (13H, m), 3.60−3.64 (2H, m), 4.69 (4H, s), 5.17 (2H, s), 8.01−9.37 (17H, m). ^{13}C NMR (DMSO-d_6, 75 MHz): δ 13.8, 19.2, 22.8, 28.0, 29.0, 30.6, 30.9, 33.1, 60.7, 61.2, 69.8, 70.8, 123.0, 124.0, 125.0, 125.7, 125.8, 126.8, 126.9, 126.9, 127.1, 127.4, 127.5, 127.7, 127.9, 130.9, 131.1, 145.8, 146.1. HRMS (ESI) Calcd for $C_{36}H_{38}N_2OBr$: 594.6038. Found: 594.6032. Anal. Calcd for $C_{36}H_{38}Br_2N_2O$: C, 64.10; H, 5.68; N, 4.15. Found: C, 64.19; H, 5.91; N 4.02.

2.6. Synthesis of {*N*-(Butyl)-*N*′-[10-(1-pyrenylmethoxy)dec-1-yl]}-4,4′-bipyridinium Dibromide (PYL12V^{2+}). To a stirred suspension of sodium hydride (19 mmol) in dry THF (10 mL) under reflux condition was added a solution of 1-(hydroxymethyl)pyrene (1 mmol) and 1,10 dibromodecane (5 mmol) over a period of 30 min in dry THF (20 mL). The reaction mixture was refluxed for 24 h, and excess sodium hydride was quenched with water. The organic layer was extracted with dichloromethane. Removal of the solvent under reduced pressure gave the product, which was purified by recrystallization from a mixture (2:8) of ethyl acetate and hexane, in a 42% yield, mp 54−55 °C. ^{1}H NMR ($CDCl_3$, 300 MHz): δ 1.20−1.80 (16H, m), 3.35−3.40 (2H, m), 3.58−3.62 (2H, m), 5.21 (2H, s), 8.01−8.40 (9H, m). ^{13}C NMR ($CDCl_3$, 75 MHz): δ 25.0, 25.8, 26.2, 28.7, 29.2, 29.4, 29.9, 32.6, 33.7, 70.1, 76.6, 115.8, 123.5, 125.5, 125.2, 125.9, 126.9, 127.4, 127.7.

To a solution of 10-bromodecyl-1-methylpyrene ether (0.5 mmol) in dry acetonitrile (30 mL), 1-butyl-4,4′-bipyridinium bromide (0.5 mmol) was added and stirred for 12 h at room temperature. Precipitated product was filtered and dried in a vacuum oven to give the compound, which was then recrystallized from a mixture (7:3) of methanol and ethyl acetate, in a 29% yield, mp 217−218 °C. ^{1}H NMR (DMSO-d_6, 300 MHz): δ 1.15−2.08 (23H, m), 3.55−3.59 (2H, m), 4.65−4.69 (4H, m), 5,17 (2H, s), 8.09−9.33 (17H, m). ^{13}C NMR (DMSO-d_6, 75 MHz): δ 12.5, 18.1, 24.7, 25.0, 27.6, 27.9, 28.1, 28.6, 29.9, 31.9, 60.3, 69.0, 69.7, 122.9, 123.3, 123.4, 123.9, 124.5, 125.6, 125.9, 126.6, 126.5, 126.7, 128.0, 128.9, 129.7, 131.6, 145.0, 146.0, 148.0. HRMS (ESI) Calcd for $C_{41}H_{48}N_2OBr$: 664.7367. Found: 664.7360. Anal. Calcd for $C_{41}H_{48}Br_2N_2O$: C, 66.13; H, 6.50; N, 3.76. Found: C, 66.29; H, 6.33; N, 3.89.

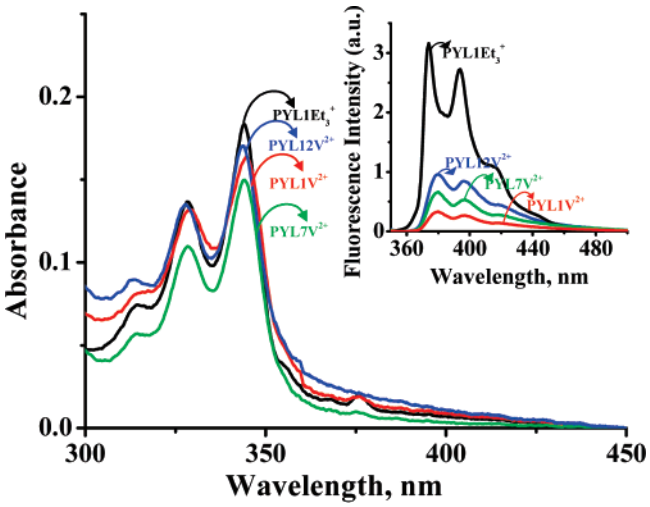

Figure 2. Absorption spectra of **PYL1V**$^{2+}$ (0.56×10^{-5} M), **PYL7V**$^{2+}$ (0.55×10^{-5} M), **PYL12V**$^{2+}$ (0.5×10^{-5} M), and the model compound **PYL1Et$_3$**$^+$ (0.51×10^{-5} M) in phosphate buffer (10 mM, pH 7.4) containing 2 mM NaCl. Inset: Fluorescence emission spectra of **PYL1V**$^{2+}$, **PYL7V**$^{2+}$, **PYL12V**$^{2+}$ (multiplied by a factor of 25 for clarity) and the model compound **PYL1Et$_3$**$^+$ in phosphate buffer (pH 7.4). The excitation wavelength was 340 nm.

3. Results

3.1. Synthesis and Photophysical Properties. The synthesis of the viologen-linked pyrene conjugates **PYL1V**$^{2+}$, **PYL7V**$^{2+}$, and **PYL12V**$^{2+}$ was achieved in moderate yields through the S_N2 reaction of the corresponding bromoalkylpyrene derivative with 1-butyl-4,4′-bipyridinium bromide. These bifunctional conjugates were purified and characterized on the basis of analytical results and spectral evidence. For example, the ^{1}H NMR spectrum of the conjugate **PYL1V**$^{2+}$ showed peaks corresponding to the quarternized methylene groups at δ 4.69 and 6.82, whereas the aliphatic protons corresponding to the butyl group appeared as multiplets in the region between δ 0.90 and δ 1.97. However, the higher conjugates **PYL7V**$^{2+}$ and **PYL12V**$^{2+}$ showed a single peak corresponding to both the quarternized methylene groups at δ 4.69, whereas the aliphatic protons corresponding to the spacer and butyl groups appeared as multiplets in the region between δ 0.94 and δ 3.64.

The viologen-linked pyrene conjugates **PYL1V**$^{2+}$, **PYL7V**$^{2+}$, and **PYL12V**$^{2+}$ and the model compound **PYL1Et$_3$**$^+$ in 10 mM phosphate buffer showed characteristic absorption spectra with a maximum at 344 nm, corresponding to the pyrene chromophore (Figure 2).

The absorption spectra of these derivatives in buffer can be described as the sum of the absorption bands of the pyrene chromophore and the viologen (MV^{2+}) moiety. There is no evidence for any ground-state charge-transfer interaction existing between the pyrene and the viologen moieties in these systems. The inset of Figure 2 shows the fluorescence emission spectra of **PYL1V**$^{2+}$, **PYL7V**$^{2+}$, and **PYL12V**$^{2+}$ and the model compound **PYL1Et$_3$**$^+$ in buffer. All these compounds show structurally similar fluorescence spectra characteristic of the pyrene chromophore with a maximum of approximately 380 nm. The fluorescence quantum yields of the viologen-linked pyrene derivatives were calculated and are found to be 2 orders of magnitude less than that of the model compound **PYL1Et$_3$**$^+$ (Table 1). For example, the model derivative **PYL1Et$_3$**$^+$ exhibited a fluorescence quantum yield of $\Phi_F = 0.32$, whereas significantly lower values of $\Phi_F = 0.0021$, 0.0044, and 0.0058, respectively, were observed for the bifunctional derivatives **PYL1V**$^{2+}$, **PYL7V**$^{2+}$, and **PYL12V**$^{2+}$.

TABLE 1: Absorption (λ_{ab}), Fluorescence (λ_{em}), and DNA Binding (K_{DNA}) Properties and Binding Site Sizes (n) of PYL1Et$_3^{+}$, PYL1V^{2+}, PYL7V^{2+}, and PYL12V^{2+} in Phosphate Buffer (10 mM, pH 7.4)[a]

compound	λ_{ab}/nm (ϵ/M^{-1}cm^{-1})	λ_{em}/nm (Φ_f[a] $\times$ 10^2)	k_{ET}[b]/s^{-1}	K_{DNA}[c]/M^{-1}	n
PYL1Et$_3^{+}$	344 (24090)	374 (32 $\pm$ 0.1)	-	2.6 $\times$ 10^4	1.9 $\pm$ 0.3
PYL1V^{2+}	344 (22650)	380 (0.21 $\pm$ 0.01)	3.2 $\times$ 10^9	1.1 $\times$ 10^4	1.4 $\pm$ 0.2
PYL7V^{2+}	344 (19170)	380 (0.44 $\pm$ 0.07)	1.5 $\times$ 10^9	1.9 $\times$ 10^4	1.7 $\pm$ 0.2
PYL12V^{2+}	344 (28730)	380 (0.58 $\pm$ 0.09)	1.1 $\times$ 10^9	2.3 $\times$ 10^4	1.8 $\pm$ 0.3

[a] The data are the average of more than two independent experiments, and the error is ca. $\pm$5%. [b] Intramolecular electron-transfer rate constants are determined using the fluorescence lifetime of the model derivative **PYL1Et$_3^{+}$** in the buffer (τ = 118.8 ns). [c] Calculated as reported in ref 17.

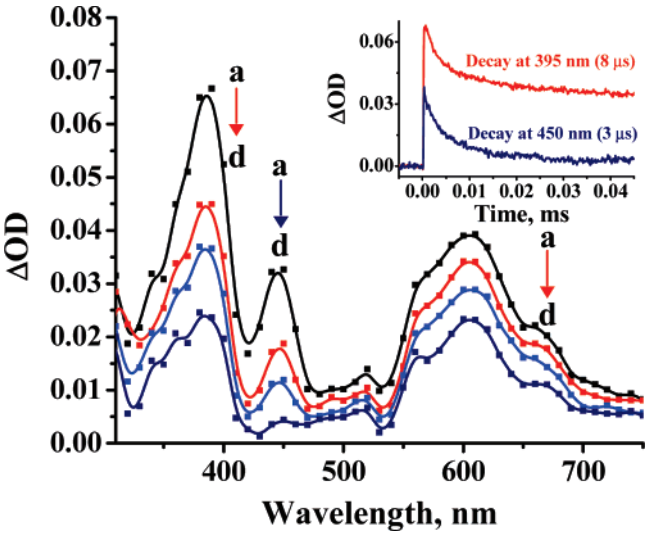

Figure 3. Transient absorption spectra of 1-(hydroxymethyl)pyrene (5×10^{-5} M) in the presence of viologen (MV^{2+}, 5×10^{-5} M) in methanol recorded at (a) 7, (b) 10, (c) 20, and (d) 55 ms after 355 nm laser excitation. Inset: Decay of the pyrene radical cation at 450 nm and decay of the reduced viologen radical cation at 395 nm.

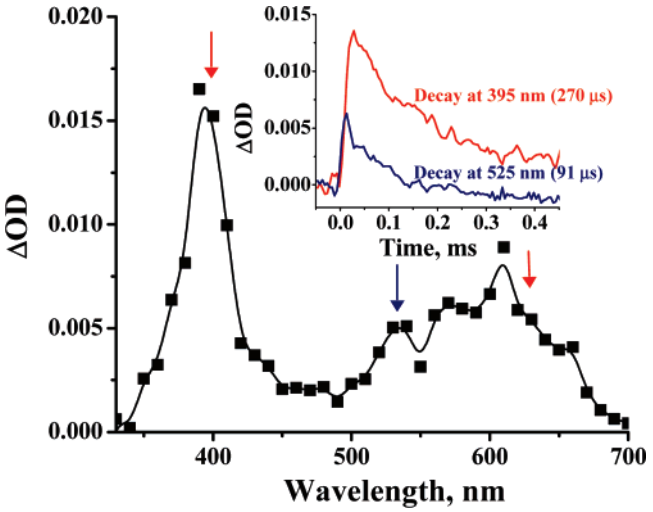

Figure 4. Transient absorption spectrum of **PYL1V^{2+}** (3.6×10^{-5} M) in the presence of guanosine (1 mM) in methanol recorded at 2 μs after 355 nm laser excitation. Inset: Decay of the reduced viologen radical cation at 395 nm and the guanosine radical cation at 525 nm.

3.2. Electron-Transfer Studies. The feasibility of photoinduced electron transfer between the pyrene chromophore and the viologen moiety (MV^{2+}) was evaluated through photophysical studies and theoretical calculations. The fluorescence emission spectrum of 1-(hydroxymethyl)pyrene in methanol showed a significant quenching with increasing concentration of MV^{2+} (Figure S1, Supporting Information). From the titration data, the bimolecular quenching rate constant (k_q) was calculated and is found to be 2×10^9 M^{-1} s^{-1}. To understand the mechanism of quenching and to characterize the transient intermediates involved, we have carried out laser flash photolysis studies under different conditions. For example, Figure 3 shows the transient absorption spectrum obtained immediately after laser excitation (355 nm, pulse width 20 ns) of 1-(hydroxylmethyl)pyrene in methanol and in the presence of MV^{2+}. On the basis of quenching experiments with molecular oxygen, the transient species having an absorption maximum at 450 nm and a lifetime of 3 μs could be assigned to the radical cation of the pyrene chromophore. As per the literature evidence,[19] the other transient with two absorption maxima at 395 and 610 nm could be due to the reduced viologen radical cation. Interestingly, the reduced viologen radical cation thus formed is found to be quite stable in methanol under argon atmosphere. The inset of Figure 3 shows the decay of the radical cation of pyrene moiety and the decay of the reduced viologen radical cation under argon-saturated conditions. In support of the experimental observations, we calculated the change in free energy for the electron-transfer reaction, using redox potentials and the singlet excited-state energy of the pyrene chromophore,[20] which is found to be $\Delta G_{ET} = -1.59$ eV in the aqueous medium.

In electron-transfer-mediated DNA modifications, the oxidation of DNA bases by various sensitizers plays a major role. To understand their mechanism and efficacy as DNA oxidizing agents, we have investigated the bimolecular quenching properties of the viologen-linked pyrene derivatives with various DNA nucleosides. With increases in concentration of nucleosides such as guanosine, adenosine, thymidine, and cytidine (Figures S2–S5, Supporting Information), we observed negligible changes in the fluorescence emission spectra of **PYL1V^{2+}**. Similar observations were made for the other derivatives **PYL7V^{2+}** and **PYL12V^{2+}**. In contrast, the titration with strong electron donors, such as triethanolamine, led to the significant fluorescence quenching of **PYL1V^{2+}** (Figure S6, Supporting Information). From the corresponding Stern–Volmer (inset of Figure S6) plot, we obtained a high rate of electron transfer $k_{ET} = 1 \times 10^{10}$ M^{-1} s^{-1} for the reaction between triethanolamine and **PYL1V^{2+}**.

3.3. Direct Observation of Radical Cations of Guanosine and DNA. Laser flash photolysis experiments were carried out under different conditions to characterize the transient intermediates involved in these systems. The direct excitation of the viologen-linked pyrene conjugates (355 nm, pulse width 20 ns) in buffer or methanol did not show any transients. However, in the presence of an external donor such as guanosine or CT DNA, characteristic transient absorptions due to the redox species were observed. For example, Figure 4 shows the transient absorption spectrum obtained on laser excitation of **PYL1V^{2+}** in methanol and in the presence of guanosine (1 mM). This spectrum exhibited three absorption maxima at 395, 525, and 610 nm and consisted of two transient species as shown in the inset of Figure 4. The first transient with two maxima at 395 and 610 nm exhibited first-order decay with a rate constant of 3.6×10^3 s^{-1}, which could be assigned to the reduced viologen radical

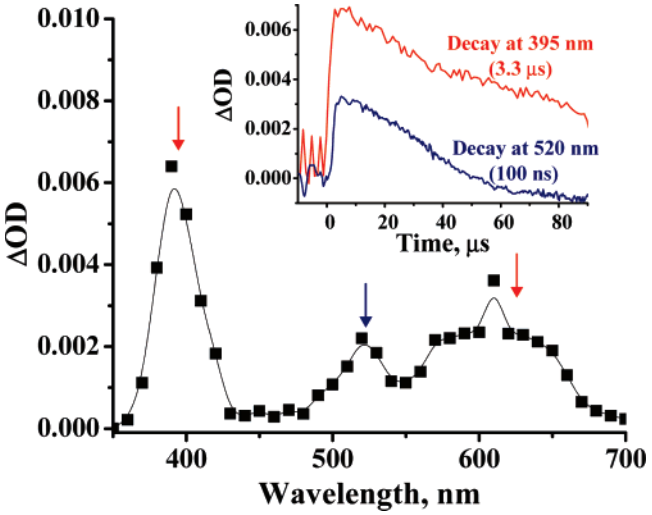

Figure 5. Transient absorption spectrum of **PYL12V**$^{2+}$ (2.5×10^{-4} M) in the presence of CT DNA (0.68 mM) in a 9:1 phosphate buffer (10 mM, pH 7.4)/methanol mixture recorded at 5 μs after 355 nm laser excitation. Inset: Decay of the reduced viologen radical cation at 395 nm and the DNA radical cation at 520 nm.

cation,[19] whereas the second transient species with absorption maximum at 525 nm exhibited first-order decay with a rate constant of 1.1×10^4 s^{-1}. As per the literature evidence,[21] the latter species could be due to the formation of the guanosine radical cation. Similar transients were obtained with the viologen-linked pyrene conjugates **PYL7V**$^{2+}$ and **PYL12V**$^{2+}$. However, the model derivative **PYL1Et$_3$**$^+$ in the presence of guanosine in methanol showed transient absorption at 420 nm with a decay rate constant of 2.3×10^4 s^{-1} (Figure S7, Supporting Information). On the basis of quenching experiments with molecular oxygen, this transient species could be assigned to the triplet excited state of the pyrene chromophore. No transient absorption corresponding to the guanosine radical cation at 525 nm was observed with the model compound **PYL1Et$_3$**$^+$.

Figure 5 shows the transient absorption spectrum obtained on laser excitation of **PYL12V**$^{2+}$ in the presence of DNA (0.68 mM) in phosphate buffer (10 mM, pH 7.4) containing 10% methanol. As in the case of guanosine, the spectrum consisted of two transient species. The transient absorption with two maxima at 395 and 610 nm corresponding to the radical cation of viologen exhibited a first-order decay rate constant of 3.0×10^5 s^{-1} with a lifetime of 3.3 μs. The other transient with an absorption maximum at 520 nm exhibited a first-order decay rate of 8.9×10^6 s^{-1} with a lifetime of 0.1 μs. This species could be assigned to the formation of radical cation of DNA wherein the radical center is located at the guanine moiety in DNA, as per the literature reports.[21] The formation of the radical cations of both reduced viologen and DNA in the presence of CT DNA indicates that the viologen-linked pyrene conjugates are capable of oxidizing DNA efficiently.

3.4. DNA Binding Properties. To understand how efficiently these bifunctional conjugates interact with DNA, we investigated their DNA binding properties using absorption, fluorescence, viscometry, and circular dichroism (CD) techniques. As shown in Figure 6, the addition of DNA to a solution of **PYL1V**$^{2+}$ resulted in a gradual decrease in the absorbance at 345 nm, corresponding to the pyrene chromophore. The maximum hypochromism (~50%) was observed at 0.08 mM DNA and with the formation of a new band at 355 nm. The corresponding fluorescence spectra are shown in the inset of Figure 6, which showed negligible changes with increases in the concentration

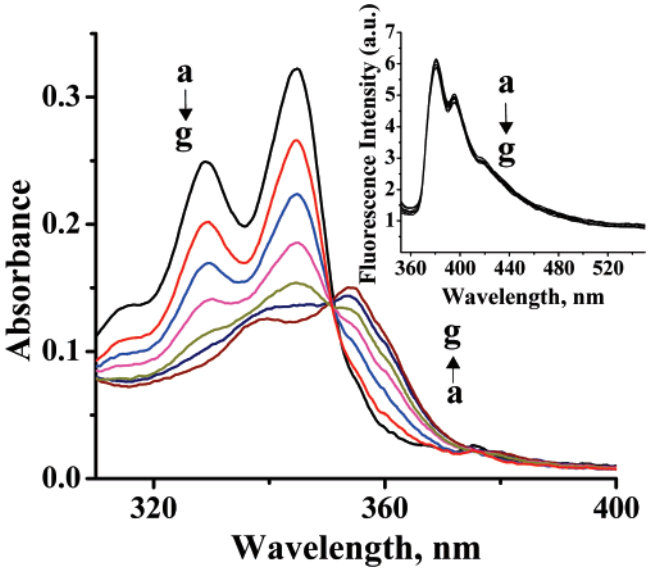

Figure 6. Absorption spectra of **PYL1V**$^{2+}$ (1.1×10^{-5} M) in the presence of CT DNA in phosphate buffer (10 mM, pH 7.4) containing 2 mM NaCl: [DNA] (a) 0, (b) 0.012, (c) 0.021, (d) 0.034, (e) 0.045, (f) 0.056, and (g) 0.08 mM. Inset: Corresponding changes in the fluorescence spectra. The excitation wavelength was 351 nm.

of DNA. Half-reciprocal analysis[17] of the absorbance changes gave a linear plot (Figure S8, Supporting Information) with an intrinsic binding constant (K_{DNA}) of $(1.1 \pm 0.05) \times 10^4$ M^{-1} and a binding site size of 1.4 ± 0.2 for the compound **PYL1V**$^{2+}$. A gradual decrease in the absorption intensity of **PYL1V**$^{2+}$ was observed (inset of Figure S8, Supporting Information), which reached saturation at a high concentration of DNA (0.08 mM). Similar changes in absorption and fluorescence spectra were obtained in the cases of other conjugates **PYL7V**$^{2+}$, **PYL12V**$^{2+}$, and the model compound **PYL1Et$_3$**$^+$ (Figures S9−S11, Supporting Information) with intrinsic binding constants of 1.9, 2.3, and 2.6×10^4 M^{-1} and binding site sizes of 1.7 ± 0.2, 1.8 ± 0.3, and 1.9 ± 0.3, respectively.

With a view to understanding the mode of interaction as well as binding selectivity, we studied the interactions of the selected viologen-linked pyrene derivatives with poly(dA)·poly(dT), poly(dG)·poly(dC), and CT DNA under different salt concentrations. Addition of DNA to a solution of **PYL1V**$^{2+}$ in 10 mM phosphate buffer containing 100 and 500 mM NaCl resulted in a gradual decrease in absorbance at 345 nm, with a maximum hypochromicity (~46% and 42%, respectively) at 0.06 mM DNA. The conjugate **PYL1V**$^{2+}$, which showed $K_{DNA} = (1.1 \pm 0.05) \times 10^4$ M^{-1} in phosphate buffer containing 2 mM NaCl, exhibited a marginal decrease in values of $K_{DNA} = 0.9$, 0.84, and $0.66 \pm 0.04 \times 10^4$ M^{-1}, respectively, at 50, 100, and 500 mM NaCl. From the values of K_{DNA} obtained for **PYL1V**$^{2+}$ at different salt concentrations (Figure S12, Supporting Information), we calculated the value of counterion release to be 0.09 per molecule. The nonelectrostatic contribution to the change in free energy (ΔG) of association at 300 K is calculated to be −23.1 kJ/mol, which is in agreement with the reported value for the intercalating dyes such as ethidium bromide.[18] Figure 7 shows the effect of polynucleotide, such as poly(dG)·poly(dC), concentration on the absorption spectra of **PYL1V**$^{2+}$, whereas the inset of Figure 7 shows the corresponding half-reciprocal plot. In the case of **PYL1V**$^{2+}$, we observed significant hypochromicity with increases in the concentration of poly(dG)·poly(dC), whereas only a marginal decrease in absorbance was observed with poly(dA)·poly(dT) (Figure S13, Supporting Information). From the half-reciprocal plots, we calculated the

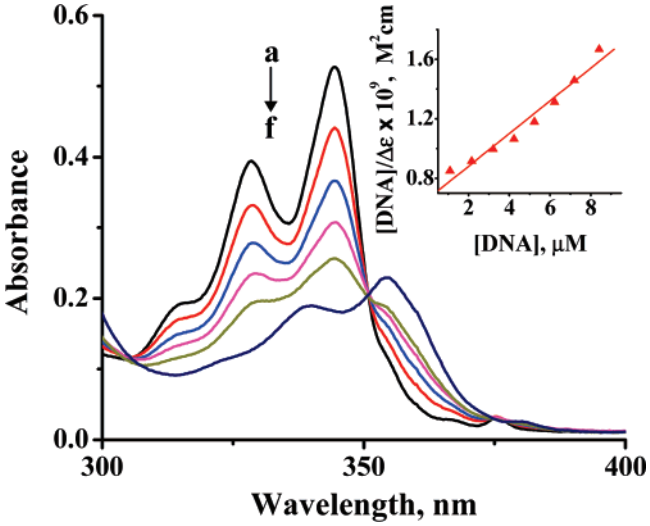

Figure 7. Absorption spectra of **PYL1V**$^{2+}$ (1.9×10^{-5} M) in the presence of poly(dG)·poly(dC) in phosphate buffer (10 mM, pH 7.4) containing 2 mM NaCl: [poly(dG)·poly(dC)] (a) 0, (b) 0.002, (c) 0.004, (d) 0.006, (e) 0.008, and (f) 0.009 mM. Inset: Corresponding half-reciprocal plot of **PYL1V**$^{2+}$.

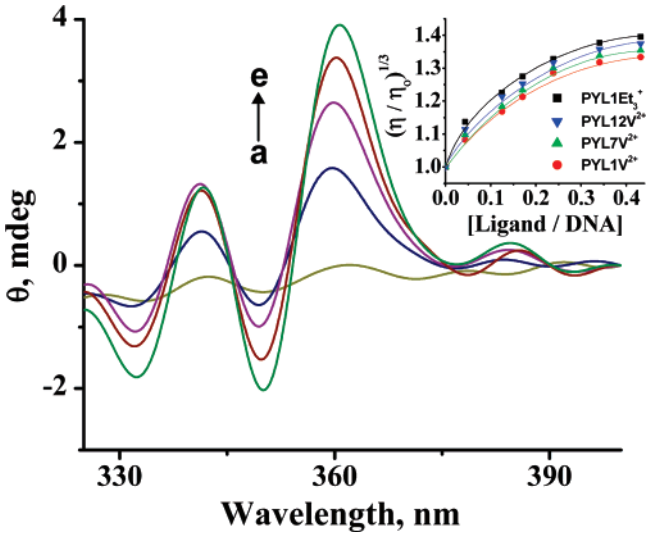

Figure 8. Circular dichroism spectra of CT DNA (0.9 mM) in the (a) absence and (b−e) presence of **PYL1V**$^{2+}$: [**PYL1V**$^{2+}$] (a) 0.34, (b) 0.09, (c) 0.17, (d) 0.26, and (e) 0.34 mM. Inset: Effect of increasing concentrations of the viologen-linked conjugates **PYL1V**$^{2+}$, **PYL7V**$^{2+}$, **PYL12V**$^{2+}$, and **PYL1Et$_3$**$^{+}$ on the relative viscosity of CT DNA (0.88 mM) at 25 ± 0.2 °C in phosphate buffer (10 mM, pH 7.4).

binding constants, which are found to be $K_{DNA} = (1.65 \pm 0.06) \times 10^4$ and $(0.84 \pm 0.03) \times 10^4$ M^{-1} for poly(dG)·poly(dC) and poly(dA)·poly(dT), respectively.

Further confirmation on the mode of interaction of the viologen-linked pyrene derivatives with DNA was demonstrated using CD and viscometric studies. Upon addition of **PYL1V**$^{2+}$ to a solution of DNA, we observed a positively bisignated induced CD signal at 360 nm corresponding to the pyrene moiety (Figure 8). Similar observations were made in the case of the conjugates **PYL7V**$^{2+}$ and **PYL12V**$^{2+}$. The observation of a bisignated CD signal in these cases is inconsistent with ligands that interact with DNA purely through an intercalative binding mode. The inset of Figure 8 shows the change in the viscosity of DNA with an increase in addition of the viologen-linked pyrene derivatives. Results indicate that the relative viscosity of DNA increases proportionally with the binding affinity of the derivatives as observed from the absorption studies. The derivative with the longer spacer length, **PYL12V**$^{2+}$, showed a maximum increase in the relative viscosity of DNA when compared to the conjugates **PYL7V**$^{2+}$ and **PYL1V**$^{2+}$.

4. Discussion

The photophysical studies of the novel bifunctional viologen-linked pyrene derivatives indicate that they exhibit low fluorescence quantum yields when compared to the model compound **PYL1Et$_3$**$^{+}$. The observed values demonstrate that the interaction between pyrene and viologen moieties is at its maximum for the conjugate **PYL1V**$^{2+}$ with $n = 1$ and decreases with increasing spacer length ($n = 7$ and 12). The calculated change in free energy values and the formation of the radical cation of the pyrene chromophore and reduced viologen moiety indicate that the excited state of the pyrene chromophore is an efficient electron donor to the viologen moiety. The observed rate of electron transfer of $k_{ET} = 3.2 \times 10^9$ s^{-1} for **PYL1V**$^{2+}$ ($n = 1$) and ca. 3 times lower value of $k_{ET} = 1.1 \times 10^9$ s^{-1}, for **PYL12V**$^{2+}$ ($n = 12$) indicate that the rate of the intramolecular electron-transfer reaction decreases with increasing spacer length (Table 1).

As per the calculated change in free energy values for the electron-transfer reaction between nucleobases and the pyrene derivatives ($\Delta G_{ET} = -0.03$, 0.13, 0.33, and 0.46 eV, respectively for G, A, C, and T),[22] we observed negligible quenching of fluorescence of the viologen-linked pyrenes with the addition of the nucleobases.[23−25] This clearly demonstrates that the viologen-linked pyrene derivatives under investigation can neither be reduced nor oxidized by the nucleobases directly. However, a strong electron donor such as triethanolamine is quite efficient in reducing these derivatives as demonstrated from the fluorescence quenching observed when triethanolamine was added. This is in good agreement with the thermodynamically predicted change in free energy for the electron transfer from triethanolamine to the singlet excited state of the pyrene chromophore ($\Delta G_{ET} = -0.33$ eV). In the case of the viologen-linked pyrene derivatives, the rate of charge separation k_{ET} and the rate of charge recombination are expected to be fast, and hence the reduced viologen radical cation could not be observed by a nanosecond laser flash photolysis technique. However, in the presence of external donors such as guanosine and DNA, we observed the formation of the radical cations of both guanosine and reduced viologen. This can be attributed due to the reduced rate of charge recombination ($k_{CR} = 1.1 \times 10^4$ s^{-1}) in the case of the charge-separated species formed in the presence of the guanosine in methanol, whereas in the presence of DNA in buffer, we observed relatively a higher rate of charge recombination ($k_{CR} = 8.9 \times 10^6$ s^{-1}).

Upon addition of CT DNA, a strong hypochromic effect along with a red shift of 7 nm in the absorption spectra of the viologen-linked pyrene derivatives and the model compound **PYL1Et$_3$**$^{+}$ was observed. This could be attributed to the $\pi-\pi$ stacking of the pyrene chromophore between DNA bases through intercalation. This interpretation is based on the experimental evidence and literature reports.[26] The fluorescence spectra of the viologen-linked pyrene derivatives showed negligible changes in the presence of DNA, indicating thereby negligible electron transfer from the DNA to the viologen-linked pyrene derivatives and vice versa from the singlet excited state. The observation of negligible changes in DNA association constants of the viologen-linked pyrenes upon increasing ionic strength of the medium from 2 to 500 mM and −23.1 kJ/mol of nonelectrostatic contribution to the change in free energy clearly suggests that these molecules undergo predominantly intercalative interactions

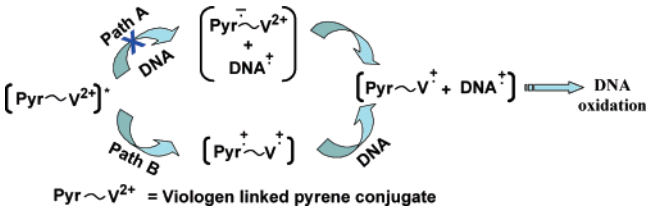

Figure 9. Schematic representation of the DNA oxidation pathways induced by the photoactivated bifunctional viologen-linked pyrene conjugates.

with DNA. The calculation of association constants between viologen-linked pyrene conjugates and DNA indicated a spacer-length-dependent increase in association constants due to the steric constraints of the viologen moiety arising from the proximity. Furthermore, the increase in the values of DNA association constants indicates that the spacer length between the pyrene chromophore and the viologen moiety play a major role in the stabilization of such DNA−ligand complexes.[17b] The observation of an increase in DNA viscosity in the presence of the bifunctional conjugates,[27] a bisignated induced CD signal corresponding to the pyrene chromophore in the presence of DNA, and a decrease in K_{DNA} values with increasing ionic strength of the buffer confirm that these systems undergo both intercalative and electrostatic interactions with DNA.[28]

Considering the electron-transfer processes in the presence of DNA, two pathways can be proposed for the oxidation of DNA by the viologen-linked pyrenes (Figure 9). Of these two pathways, path A involves first electron transfer from the DNA bases to the excited state of the pyrene chromophore, followed by transfer of an electron from the pyrene radical anion to the viologen moiety. This pathway can be ruled out in the case of the viologen-linked pyrene conjugates because of the calculated unfavorable change in free energy values for such an electron-transfer reaction and the observed negligible fluorescence quenching with various nucleobases. However, path B involving first electron transfer from the excited state of the pyrene chromophore to the viologen moiety, followed by second electron transfer from the DNA base (preferable from guanine) to the radical cation of the pyrene, is expected to be the exclusive pathway for the oxidation of DNA by these systems. This interpretation is in agreement with (i) the theoretically calculated favorable change in free energy values ($\Delta G = -1.59$ eV), (ii) the observation of efficient fluorescence quenching by the viologen moiety, and (iii) the formation of the radical cations of both reduced viologen and guanosine in the presence of the sacrificial donors such as guanosine and DNA. Interestingly, the first electron-transfer reaction in path B leads to the formation of radical cations of both pyrene and viologen moieties, which then lead to the formation of the charge-separated radical cations of both DNA and the reduced viologen moiety. The radical cation of DNA thus formed leads to DNA damage and eventually cleavage of DNA.

5. Conclusion

We observed that the pyrene chromophore in the case of the viologen-linked bifunctional systems **PYL1V**$^{2+}$, **PYL7V**$^{2+}$, and **PYL12V**$^{2+}$ constitutes an interesting variation, which controls both DNA binding and electron-transfer pathways for the oxidation of DNA. Results of these investigations demonstrate that these systems undergo predominantly intercalative interactions with DNA and exhibit 2:1 preference for poly(dG)·poly(dC) over poly(dA)·poly(dT) sequences. Theoretically calculated favorable changes in free energy values, negligible fluorescence quenching with various nucleobases, and formation of the radical cations of both reduced viologen and DNA confirm that these systems undergo first electron transfer exclusively from the excited state of the pyrene chromophore to the viologen moiety. Subsequently, a second electron transfer occurs from the DNA bases (preferably guanosine) to the radical cation of the pyrene, which results in the formation of the charge-separated radical cations of both DNA and the reduced viologen moiety. These novel bifunctional systems, which are stable in aqueous medium and efficient in oxidizing guanosine and DNA, can have potential use as photoactivated DNA cleaving agents that function purely through a cosensitization mechanism.

Acknowledgment. This work is dedicated to Professor Dr. Waldemar Adam on the occasion of his 70th birthday. Financial support from the Regional Research Laboratory (RRL), Council of Scientific and Industrial Research, Trivandrum, and the Department of Science and Technology, Government of India, is gratefully acknowledged. This is Contribution No. PPD-175 from the RRL, Trivandrum.

Supporting Information Available: Effects of CT DNA, nucleosides, and triethanolamine on absorption and fluorescence spectra of the viologen-linked pyrene conjugates **PYL1V**$^{2+}$, **PYL7V**$^{2+}$, and **PYL12V**$^{2+}$ and the model compound **PYL1Et$_3$**$^{+}$. This material is available free of charge via the Internet at http://pubs.acs.org.

References and Notes

(1) (a) Waring, M. J. In *Drug Action at the Molecular Level*; Roberts, G. K., Ed.; Macmillan: London, 1977; pp 167−189. (b) Lambert, B.; LePecque, J.-B. In *DNA−Ligand Interactions: From Drugs to Proteins*; Guschlbauer, W., Saenger, W., Eds.; Plenum: New York, 1986; p 141. (c) Pullman, B.; Jortner, J. In *Molecular Basis of Specificity in Nucleic Acid−Drug Interactions*; CRC Press: Ann Arbor, MI, 1993; Vol. 1. (d) Bischofberger, N.; Shea, R. G. In *Nucleic Acid Targeted Drug Design*; Propst, C. L., Perun, T. J., Eds.; Marcel Dekker: New York, 1992; pp 579−612. (e) *Small Molecule DNA and RNA Binders*; Demeunynck, M., Bailly, C., Wilson, W. D., Eds.; Wiley-VCH: Weinheim, Germany, 2003.

(2) (a) Tidd, D. M. In *Molecular Aspects of Anticancer Drug−DNA Interactions*; Neidle, S., Waring, M., Eds.; CRC Press: Boca Raton, FL, 1993; Vol. 1, pp 272−300. (b) Arkin, M. R.; Stemp, E. D. A.; Turro, C.; Turro, N. J.; Barton, J. K. *J. Am. Chem. Soc.* **1996**, *118*, 2267−2274. (c) Nielsen, P. E. *Bioconjugate Chem.* **1991**, *2*, 1−12. (d) Rajski, S. R.; Williams, R. M. *Chem. Rev.* **1998**, *98*, 2723−2796. (e) Brun, A. M.; Harriman, A. *J. Am. Chem. Soc.* **1994**, *116*, 10383−10393. (f) Nakatani, K.; Sando, S.; Saito, I. *J. Am. Chem. Soc.* **2000**, *122*, 2172−2177. (g) Adam, W.; Cadet, J.; Dall'Acqua, F.; Epe, B.; Ramaiah, D.; Saha-Moller, C. R. *Angew. Chem., Int. Ed. Engl.* **1995**, *34*, 107−110. (h) Duarte, V.; Gasparutto, D.; Yamaguchi, L. F.; Ravanat, J.-L.; Martinez, G. R.; Madeiros, M. H. G.; Di Mascio, P.; Cadet, J. *J. Am. Chem. Soc.* **2000**, *122*, 12622−12628. (i) Ravanat, J.-L.; Mascio, P. D.; Martinez, G. R.; Medeiros, M. H. G.; Cadet, J. *J. Biol. Chem.* **2000**, *275*, 40601−40604.

(3) (a) Schuster, G. B. *Acc. Chem. Res.* **2000**, *33*, 253−260. (b) Breslin, D. T.; Schuster, G. B. *J. Am. Chem. Soc.* **1996**, *118*, 2311−2319. (c) Armitage, B.; Yu, C.; Devadoss, C.; Schuster, G. B. *J. Am. Chem. Soc.* **1994**, *116*, 9847−9859.

(4) (a) Bohne, C.; Faulhaber, K.; Giese, B.; Hafner, A.; Hofmann, A.; Ihmels, H.; Kohler, A.-K.; Pera, S.; Scheider, F.; Sheepwash, M. A. L. *J. Am. Chem. Soc.* **2005**, *127*, 76−85. (b) Giese, B. *Acc. Chem. Res.* **2000**, *33*, 631−636. (c) Meggers, E.; Beyerle, M. E. M.; Giese, B. *J. Am. Chem. Soc.* **1998**, *120*, 12950−12955.

(5) Armitage, B. *Chem. Rev.* **1998**, *98*, 1171−1200.

(6) (a) Pogozelski, W.; Tullius, T. *Chem. Rev.* **1998**, *98*, 1089−1107. (b) Burrows, C. J.; Muller, J. G. *Chem. Rev.* **1998**, *98*, 1109−1152.

(7) Johnston, D. H.; Thorp, H. H. *J. Phys. Chem.* **1996**, *100*, 13837−13843.

(8) (a) Choi, S.; Cooley, R. B.; Hakemian, A. S.; Larrabee, Y. C.; Bunt, R. C.; Maupas, S. D.; Muller, J. G.; Burrows, C. J. *J. Am. Chem. Soc.* **2004**, *126*, 591−598. (b) Fromherz, P.; Rieger, B. *J. Am. Chem. Soc.* **1986**, *108*, 5361−5362.

(9) Dunn, D. A.; Lin, V. H.; Kochevar, I. E. *Biochemistry* **1992**, *31*, 11620−11625.

(10) (a) Rogers, J. E.; Weiss, S. J.; Kelly, L. A. *J. Am. Chem. Soc.* **2000**, *122*, 427−436. (b) Le, T. P.; Rogers, J. E.; Kelly, L. A. *J. Phys. Chem. A* **2000**, *104*, 6778−6785. (c) Rogers, J. E.; Le, T. P.; Kelly, L. A. *Photochem. Photobiol.* **2001**, *73*, 223−229.

(11) (a) Joseph, J.; Eldho, N. V.; Ramaiah, D. *Chem.—Eur. J.* **2003**, *9*, 5926−5935. (b) Eldho, N. V.; Joseph, J.; Ramaiah, D. *Chem. Lett.* **2001**, 438−439. (c) Joseph, J.; Eldho, N. V.; Ramaiah, D. *J. Phys. Chem. B* **2003**, *107*, 4444−4450.

(12) (a) Neelakandan, P. P.; Hariharan, M.; Ramaiah, D. *Org. Lett.* **2005**, *7*, 5765−5768. (b) Arun, K. T.; Ramaiah, D. *J. Phys. Chem. A* **2005**, *109*, 5571−5578. (c) Arun, K. T.; Epe, B.; Ramaiah, D. *J. Phys. Chem. B* **2002**, *106*, 11622−11627. (d) Neelakandan, P. P.; Hariharan, M.; Ramaiah, D. *J. Am. Chem. Soc.* **2006**, *128*, 11334−11335. (e) Jisha, V. S.; Arun, K. T.; Hariharan, M.; Ramaiah, D. *J. Am. Chem. Soc.* **2006**, *128*, 6024−6025.

(13) (a) Kuruvilla, E.; Joseph, J.; Ramaiah, D. *J. Phys. Chem. B* **2005**, *109*, 21997−22002. (b) Joseph, J.; Kuruvilla, E.; Achuthan, A. T.; Ramaiah, D.; Schuster, G. B. *Bioconjugate Chem.* **2004**, *15*, 1230−1235.

(14) Roshal, A. R.; Organero, J. A.; Douhal, A. *Chem. Phys. Lett.* **2003**, *379*, 53−59.

(15) Deng, H.; Cai, J.; Xu, H.; Zhang, H.; Ji, L. *J. Chem. Soc., Dalton Trans.* **2003**, 325−330.

(16) Baguley, B. C.; Falkenhaug, E.-M. *Nucleic Acids Res.* **1978**, *5*, 161−171.

(17) (a) Kumar, C. V.; Asuncion, E. H. *J. Am. Chem. Soc.* **1993**, *115*, 8547−8553. (b) Modukuru, N. K.; Snow, K. J.; Perrin, B. S., Jr.; Thota, J.; Kumar, C. V. *J. Phys. Chem. B* **2005**, *109*, 11810−11818.

(18) Petty, J. R.; Bordelon, J. A.; Robertson, M. E. *J. Phys. Chem. B* **2000**, *104*, 7221−7227.

(19) Watanabe, T.; Honda, K. *J. Phys. Chem.* **1982**, *86*, 2617−2619.

(20) (a) The oxidation potential of pyrene is 1.28 V, the reduction potential of viologen is −0.45 V, and the singlet energy of pyrene is 3.32 V. Murov, S. L.; Carmichael, I.; Hug, G. L. In *Handbook of Photochemistry*, 2nd ed.; Marcel Dekker: New York, 1993. (b) Rehm, D.; Weller, A. *Ber. Bunsen-Ges. Phys. Chem.* **1969**, *73*, 834−836. (c) Weller, A. *Z. Phys. Chem.* **1982**, *133*, 93−98.

(21) (a) Candeias, L. P.; Steenken, S. *J. Am. Chem. Soc.* **1989**, *111*, 1094−1099. (b) Okhubo, K.; Yukimoto, K.; Fukuzumi, S. *Chem. Commun.* **2006**, 2504−2506.

(22) (a) Zahavy, E.; Fox, M. A. *J. Phys. Chem. B* **1999**, *103*, 9321−9327. (b) The reduction potential of pyrene, $Py/Py^{\bullet-}$ is −2.09 V; the oxidation potentials of the nucleobases $dG^{+\bullet}/dG$, $dA^{+\bullet}/dA$, $dC^{+\bullet}/dC$, and $dT^{+\bullet}/dT$ are 1.29, 1.42, 1.60, and 1.70 V, respectively; the reduction potentials of the nucleobases $dG/dG^{\bullet-}$, $dA/dA^{\bullet-}$, $dC/dC^{\bullet-}$, $dT/dT^{\bullet-}$, and $dU/dU^{\bullet-}$ are −2.52, −2.28, −2.11, −1.94, and −1.83 V, respectively. Steenken, S.; Telo, J. P.; Novais, H. M.; Candeias, L. P. *J. Am. Chem. Soc.* **1992**, *114*, 4701−4709.

(23) (a) Trifonov, A.; Raytchev, M.; Bucharov, I.; Rist, M.; Barbaric, J.; Wagenknecht, H.-A.; Fiebig, T. *J. Phys. Chem. B.* **2005**, *109*, 19490−19495. (b) Wagenknecht, H.-A. *Angew. Chem., Int. Ed.* **2003**, *42*, 2454−2460.

(24) (a) Seidel, C. A. M.; Schulz, A.; Sauer, H. M. *J. Phys. Chem.* **1996**, *100*, 5541−5553. (b) Telser, J.; Cruickshank, K. A.; Morrison, L. E.; Netzel, T. L.; Chan, C.-K. *J. Am. Chem. Soc.* **1989**, *111*, 7226−7232. (c) Mann, J. S.; Shibata, Y.; Meehan, T. *Bioconjugate Chem.* **1992**, *3*, 5544−558.

(25) Crean, C.; Geacintov, N. E.; Shafirovich, V. *Angew. Chem., Int. Ed.* **2005**, *44*, 5057−5060.

(26) (a) Cantor, C.; Schimmel, P. R. In *Biophysical Chemistry*; W. H. Freeman: San Fransisco, CA, 1980; Vol. 2, pp 398−413. (b) Masuko, M.; Ohtani, H.; Ebata, K.; Schimadzu, A. *Nucleic Acids Res.* **1998**, *26*, 5409−5416.

(27) (a) Reinert, K. E. *Nucleic Acids. Res.* **1983**, *11*, 3411−3430. (b) Breslin, D. T.; Coury, J. E.; Anderson, J. R.; McFail-Isom, L.; Kan, Y.; Williams, L. D.; Bottomley, L. A.; Schuster, G. B. *J. Am. Chem. Soc.* **1997**, *119*, 5043−5044.

(28) Becker, H.-C.; Norden, B. *J. Am. Chem. Soc.* **1999**, *121*, 11947−11952.